

# Simplified Analytical Determination of the Temperature Distribution and the Load Bearing Resistance of Slim-Floor Beams

Matthias Braun<sup>a,\*</sup>, Dario Zaganelli<sup>a</sup>, Francois Hanus<sup>b</sup>, Renata Obiala<sup>c</sup>,  
Louis-Guy Cajot<sup>a</sup>, Anthony Peirce<sup>d</sup>

<sup>a</sup> ArcelorMittal Europe - Long Products, L-4009 Esch sur Alzette, Luxembourg  
\* mathias.braun@arcelormittal.com

<sup>b</sup> ArcelorMittal Global R&D, L-4009 Esch sur Alzette, Luxembourg

<sup>c</sup> University of Luxembourg, Chair of Steel and Façade Engineering, L-1359 Luxembourg

<sup>d</sup> Department of Mathematics, University of British Columbia, Vancouver, British Columbia, V6T 1Z2, Canada.

## ABSTRACT

This contribution presents an analytical method to determine the distribution of temperature within a steel section integrated into a concrete slab, which is subjected to a time-dependent heat flux. The method developed is based on an analytical solution of the general heat equation for transient conduction simplified to be usable for the calculation of the load bearing resistance of the slim-floor beam. This simplified analytical solution is validated by comparison against results obtained from numerical simulations. A possible extension of the developed method to fire protected sections is given.

**Keywords:** composite slim-floor beam, CoSFB, fire resistance, heat equation, intumescent coating

## 1 INTRODUCTION

A slim-floor beam (SFB) or a slim-floor beam with composite action (CoSFB), is a floor beam which is integrated into a slab [1, 2]. It consists of a hot rolled steel section and a plate welded under the lower flange of the hot rolled section. The width of the plate is wider than the upper flange to allow for an easy installation of the slab elements, *Fig. 1*.

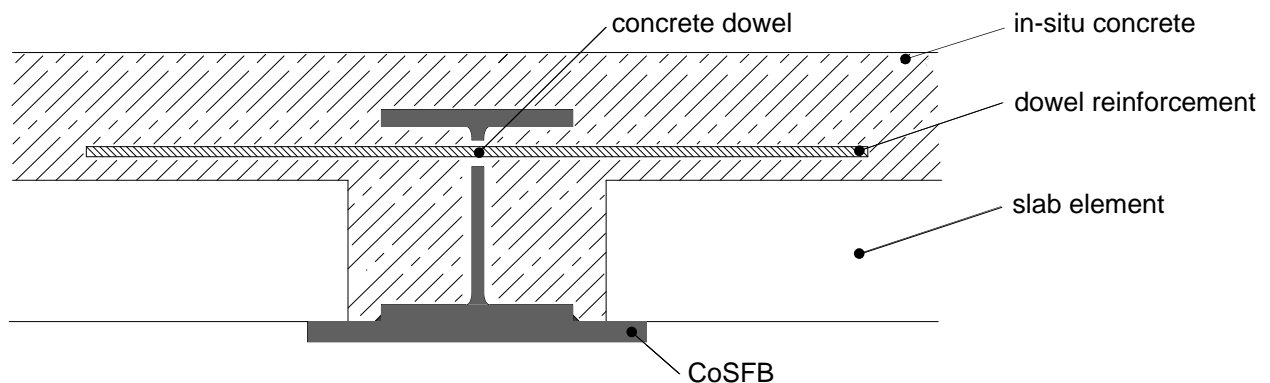


*Fig. 1. Composite Slim-Floor Beam – CoSFB [2]*

The slab may be made of partially or fully prefabricated slab elements or composite slabs with metal decking [3]. In case of a fire underneath the slab, the lower edge of the slab and the steel plate are exposed to hot gases from the fire, while that part of the steel section integrated into the slab is heated by conduction only. Hence the temperature distribution within the height of the steel section is highly non-uniform, *Fig. 2*.

No simple method to determine the temperature distribution in the steel section or to determine the load bearing resistance of a slim-floor beam can be found in Eurocode 3 or Eurocode 4 [4, 5]. In order to allow for a quick and easy design in the event of fire, a simple method to assess the fire resistance of integrated floor beams has to be developed.

The method together with recent developments of new slab systems, e.g. Cofradal 200 and Cofraplus 220 and a new type of shear connector – the “CoSFB-Betondübel” – will lead to an overall more economic and sustainable slim-floor construction [6, 7].

This contribution presents an analytical method to determine the temperature distribution of a SFB section, which is integrated into a concrete slab and subjected to a fire, defined by a temperature-time relationship. The presented method is based on an analytical solution of the general heat equation for transient conduction and simplified to be used for the calculation of the load bearing resistance of a slim-floor beam. Further, the quality of the developed method is validated by comparison with the results obtained by numerical simulations. The undeniable advantage of the chosen approach is its possible application to any type of fire protection, including a protection of the lower plate of the slim-floor section with intumescent coating.

## 2 TEMPERATURE DISTRIBUTION IN SLIM-FLOOR CROSS SECTIONS

### 2.1 Temperature distribution in SFB sections in solid concrete slabs

Temperatures obtained by numerical simulation for a SFB section are presented in Fig. 2. The lower edge of the slab and the steel plate are exposed to hot gases from the standard temperature-time curve (“ISO-Fire”) [8] and sampled at 30min (R30) and 120min (R120). In both cases the temperature is decreasing over the section height (y-direction). In addition, a gradient of the steel temperatures in the horizontal, z-direction exists at 30min, while this temperature gradient is reducing with increasing time. Compared to the concrete slab the thermal conductivity of structural steel is higher and the mass of the steel section is smaller, which leads to a higher value of the diffusivity  $\alpha$  of the steel section and consequently, it heats faster than the concrete slab (if both materials are subjected to the same heat flux). This leads to a thermal gradient between the steel section and the concrete slab and to a heat exchange between the steel section and the surrounding concrete.

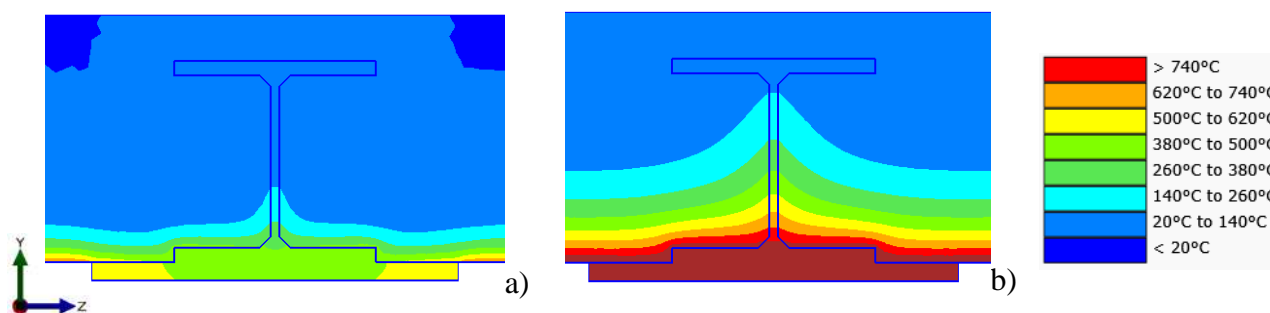


Fig. 2. Temperatures in a SFB cross section a) 30min; b) 120min

### 2.2 Description of the simplified analytical approach

Precise analytical determination of the time- and space-dependent temperature distribution in integrated beams results in a complex solution, which is less practical for beam design. Therefore, simplifications were introduced allowing for a simpler analytical formulation being adequate for the design of composite and non-composite integrated floor beams in fire. The time-dependent temperature distribution within a solid material can be formulated by a non-homogenous partial differential equation, describing the process of transient heat conduction, Section 3.

In case of fire, the surfaces exposed to the fire are directly subjected to thermal actions. These thermal actions can be formulated as a net heat flux  $\dot{h}_{\text{net}}$  to the exposed surface of the member. This heat flux includes heat transfer by radiation and convection. The key parameter for the amount of radiation and convection to a surface is the temperature difference between the surface temperature  $T_{\text{a,surf}}$  and the gas temperature [8], Fig. 3.

Up to 120min the temperature of the upper edge of the concrete slab ( $T_{\text{c,cold}}$ ) remains almost at its initial temperature ( $T_i = 20^\circ\text{C}$ ) – the slab is nearly not affected by an internal heat transport from conduction, which justifies the assumption of an adiabatic boundary condition at the upper edge.

Using the net heat flux allows us to apply the developed method for protected and un-protected slim-floor beams. If the lower plate of the slim-floor beam is protected, e.g. with intumescent coating, this fire protection material leads to a reduction of the heat flux to the steel plate and consequently to a general reduction of the steel temperature. To calculate  $\dot{h}_{net}$  for protected members the surface temperature as a function of time may be taken from fire tests. It is recommended to use test results for members with a similar section factor  $A_m/V$  [4] as the welded plate. Test results for a specific fire protection material may be provided by the producer.

The simplifications introduced for the determination of the analytical solution are:

- no thermal gradient in horizontal z-direction is taken into account (i.e., a uniform temperature in the plate and the lower flange is assumed),
- heat exchange between the steel section and the concrete is not considered,
- the developed method is valid for solid concrete slabs only,
- the temperature dependency of the specific heat  $c_a$  and the thermal conductivity  $\lambda_a$  of steel is simplified, Section 3.

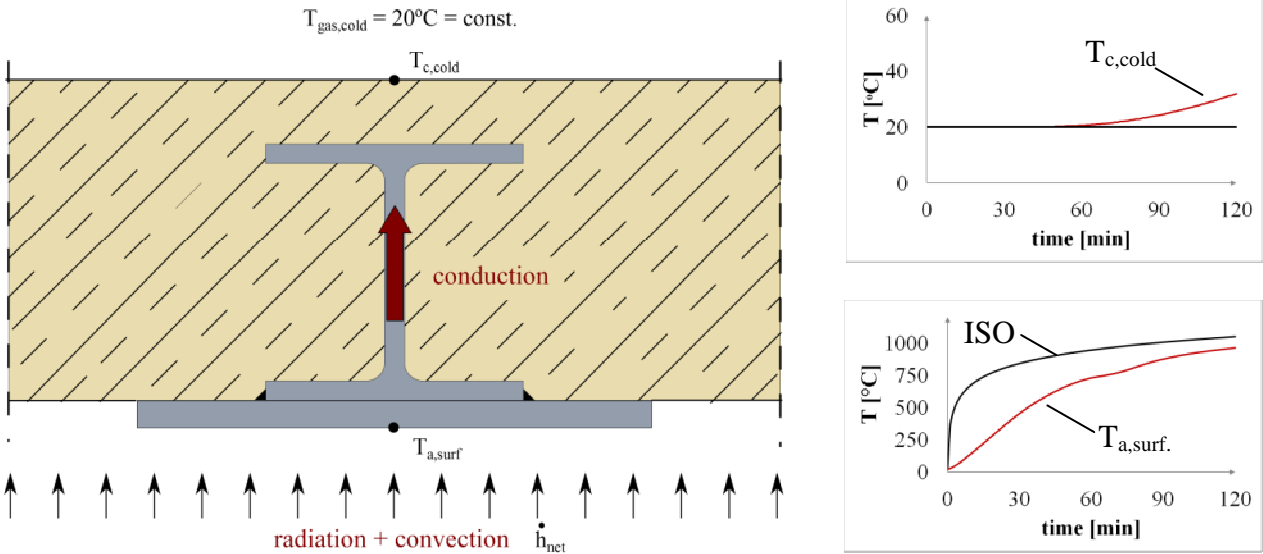


Fig. 3. Heat Flux on SFB section with surface Temperatures

**2.3 Application range**

The developed method has been derived for composite and non-composite SFB sections, Table 1.

Table 1. List of considered SFB cross sections

Hot rolled section	Plate	
	b <sub>pl</sub> [mm]	t <sub>pl</sub> [mm]
HE180B	350	20
HE200B	350	20
HE220B	400	20
HE240B	400	20
HE260B	400	20
HE280B	450	20
HE300B	500	20
HE320B	500	25
HE340B	500	25
HE360B	500	30

The steel grade of the hot rolled section and the welded plate is S355. For all sections a fixed value of the concrete cover c of 50mm above the upper flange was used, the slab consists of a solid concrete slab with concrete in compression class C30/37, Fig. 6.

### 3 ANALYTICAL FORMULATION OF THE TEMPERATURE DISTRIBUTION

#### 3.1 Differential equation of transient conduction

A slim-floor beam subjected to the action of a heat source as an ISO fire presents a highly non-uniform temperature distribution and a consequent exchange of thermal energy from regions of higher temperature to regions of lower temperature. The thermal exchange in space and time in the cross section is defined by the well-known heat transfer equation. Assuming that there is no internal heat generation in the slab and that the thermal exchange for conduction is one-dimensional, the heat equation is expressed as follows:

$$\frac{\partial^2 T}{\partial x^2} = \frac{1}{\alpha} \frac{\partial T}{\partial t} \quad 0 < x < H, t > 0 \quad (1)$$

With thermal diffusivity  $\alpha = \frac{\lambda_a}{\rho_a \cdot c_a}$  ( $\lambda_a$  is the thermal conductivity,  $\rho_a$  is the density and  $c_a$  is the specific heat of steel);  $x$  is the spatial coordinate with its origin on the hot side of the slab;  $t$  is the coordinate in time;  $H$  is the thickness of the slab and  $T$  is the temperature. In order to solve this equation one initial condition (IC) and two boundary conditions (BC) have to be defined. As shown in Section 2 an adiabatic BC can be used on the cold side. Further, the presence of a constant thermal heat flux  $q$  is defined as the BC on the side of the cross section exposed to the fire. As an IC a constant temperature of  $T_i = 20^\circ\text{C}$  is set. These conditions have been expressed as follows:

$$\text{BC1: } -\lambda_a \frac{\partial T}{\partial x} = q, \quad x = 0 \quad (2)$$

$$\text{BC2: } \frac{\partial T}{\partial x} = 0, \quad x = H \quad (3)$$

$$\text{IC: } T = T_i = 20^\circ\text{C}, \quad 0 < x < H, \quad t = 0 \quad (4)$$

In order to reduce the amount of variables a standard procedure of conversion to non-dimensional form is used by grouping the physical constants of the initial problem:

$$\theta = \frac{T - T_i}{q \cdot H / \lambda_a} \quad (5)$$

$$\text{and } X = \frac{x}{H}; \quad Fo = \frac{\alpha \cdot t}{H^2} \quad (\text{Fo can be interpreted as dimensionless time})$$

By introducing the new variables, the following non-dimensional 1D heat equation is obtained.

$$\frac{\partial^2 \theta}{\partial X^2} = \frac{\partial \theta}{\partial Fo} \quad 0 < X < 1, \quad Fo > 0 \quad (6)$$

$$\text{BC1: } \frac{\partial \theta}{\partial X} = -1, \quad X = 0 \quad (7)$$

$$\text{BC2: } \frac{\partial \theta}{\partial X} = 0, \quad X = 1 \quad (8)$$

$$\text{IC: } \theta = 0, \quad 0 < X < 1, \quad Fo = 0 \quad (9)$$

This non-homogeneous differential equation is solved by applying the method of variation of parameters, setting up a homogenous problem by eliminating the non-homogeneous BC and applying the separation of variables to get the Eigenvalues and Eigenfunctions of the homogeneous system. Using the orthogonality property of the Eigenfunctions it is then possible to solve the original non-homogeneous system. The solution for the non-dimensional heat equation is presented in Eq. (10):

$$\theta(X, Fo) = Fo + \frac{2}{\pi^2} \sum_{n=1}^{\infty} \frac{\cos(n\pi X)}{n^2} - \frac{2}{\pi^2} \sum_{n=1}^{\infty} \frac{\cos(n\pi X)}{n^2} e^{-(n\pi)^2 Fo} \quad (10)$$

The above assumptions have been validated through results obtained by extensive finite element simulations, considering different slim-floor beam geometries. A dedicated finite element software developed at the University of Liège [9] has been employed for this purpose.

### 3.2 Determination of the heat flux for unprotected SFB sections

A heat flux constant over time has to be defined to enable application of  $Eq. (10)$ . The heat flux considers heat transfer by radiation and convection on the fire exposed surfaces (lower edges of the steel plate and the concrete slab). Based on the surface temperature of the steel plate obtained by numerical simulations [9] the net heat flux  $\dot{h}_{net}$  as a function of time, is calculated and presented in *Fig. 4*. All other parameters for the calculation of  $\dot{h}_{net}$  were directly taken from the Eurocodes [4, 8].

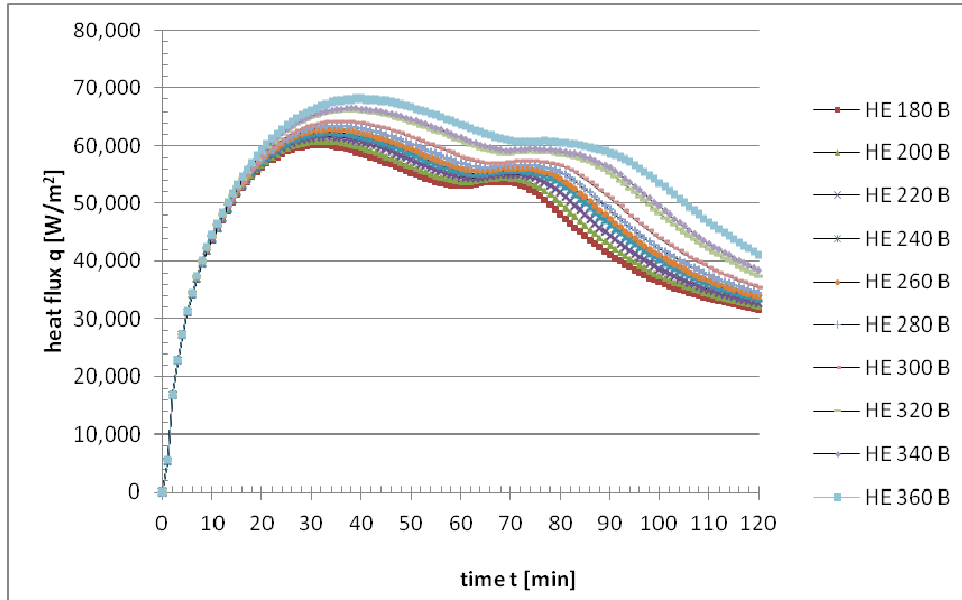


*Fig. 4. Heat flux for sections according to Table 1*

Because the temperatures and the bending resistance of the cross section is required for specific times only (R30, R60, R90, R120), the constant value of  $q$  is derived by an integration of the function of the heat flux, divided by the corresponding time. Values for the SFB section HE260B + Plate 400x20 are given in *Fig. 5*.

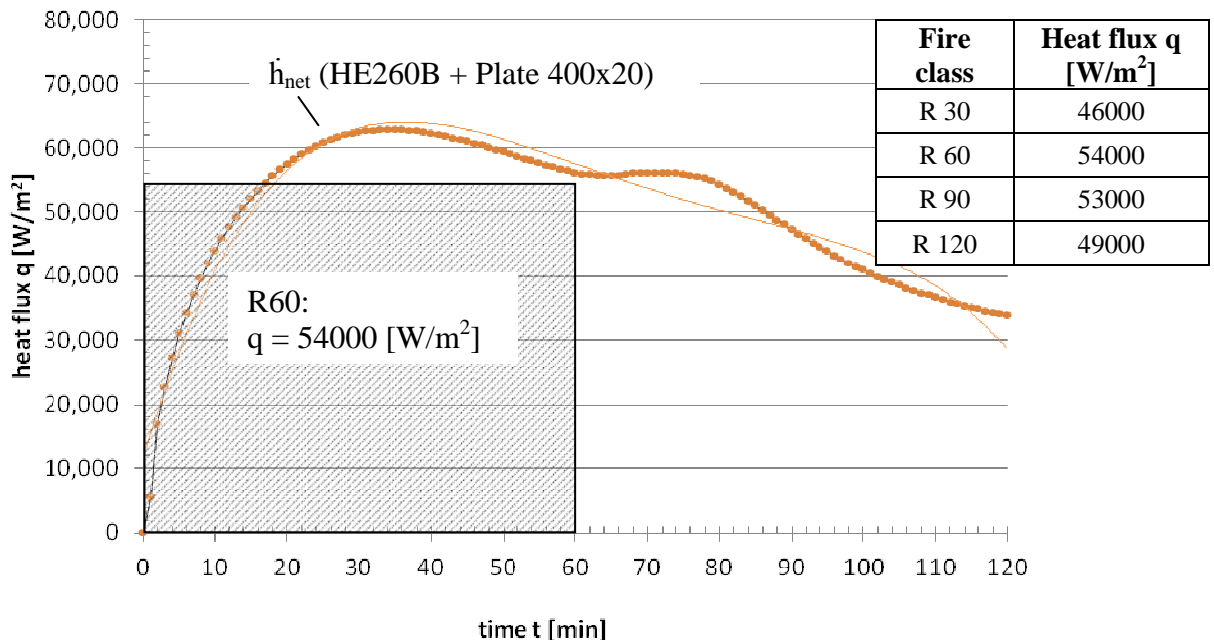


*Fig. 5. Heat flux  $q$ , for HE260B with integration example for R60 + heat flux values for R30, R60, R90 and R120*

Further, due to the small variation of the heat flux within the given range of SFB sections a net heat flux  $q'$  for all sections given in Table 1 can be derived by multiplying the heat flux  $q$  for the HE260B by a factor, *Eq. (11)*:  $q' = q * \frac{H_{HE260B}}{H_{section}}$  (11)

### 3.3 Analytical development of the non-linear temperature distribution

The dimensional values for the temperatures are obtained by reformulating Eq. (5) as follows:

$$T(X, Fo) = \theta(X, Fo) \cdot q' \cdot H / \lambda_a + T_i \tag{12}$$

Recalling Eq. (10) and Eq. (12), the temperatures at specified points within the SFB section are computed assigning to each point a non-dimensional vertical coordinate X, with origin at the lower edge of the plate upwards, and a related dimensionless time Fo. The value H, is always defined as a total height of the steel profile and the steel plate. The temperature is calculated at three significant points: Temperature T<sub>1</sub> at Point 1 placed in the centre of the plate; Temperature T<sub>2</sub> at Point 2 placed in the centre of the lower flange; Temperature T<sub>3</sub> at Point 3 placed at the upper edge of the root fillet, Fig. 6.

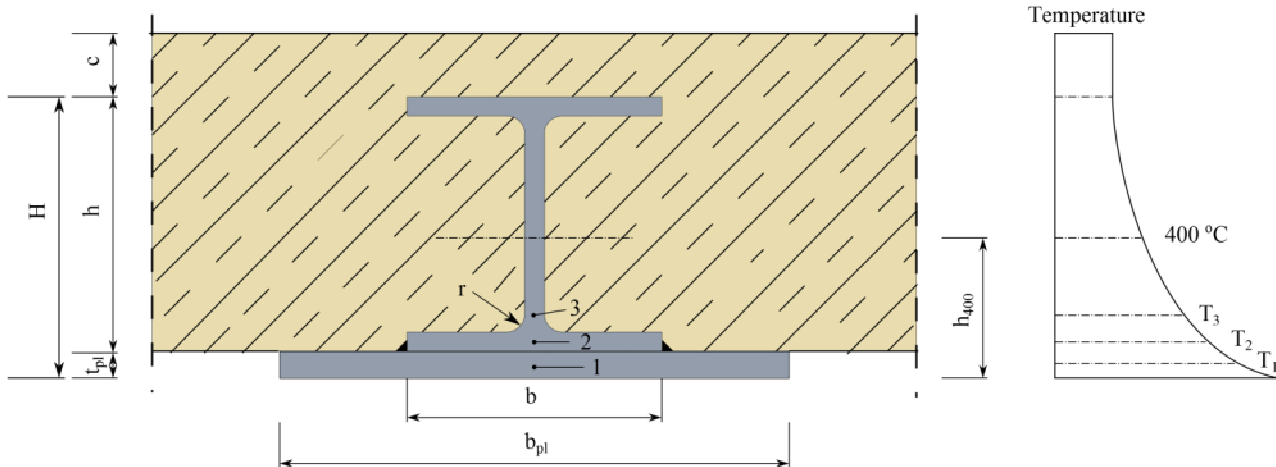


Fig. 6. SFB cross section with relevant points for Temperature calculation

Because the Fo is a function of space and time, it depends on the fire resistance class and has to be calculated individually for each of the 3 Points described above, Fig. 7.

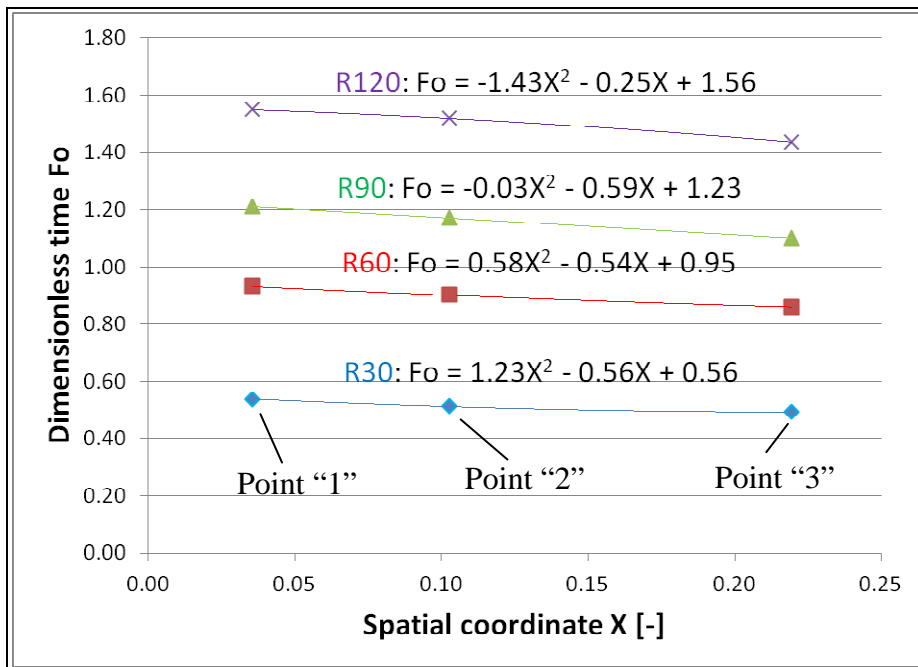


Fig. 7. Fo as function of X and the fire resistance class

With the aim to allow for the application of Eq. (10) to all sections given in Table 1, the Fo is multiplied by a geometrical coefficient, expressing the square root of the ratio between the flange thickness of the HE260B and of the chosen section.

Hence Eq. (10) is reformulated into:

$$\theta'(X, Fo) = Fo' + \frac{2}{\pi^2} \sum_{n=1}^{\infty} \frac{\cos(n\pi X)}{n^2} - \frac{2}{\pi^2} \sum_{n=1}^{\infty} \frac{\cos(n\pi X)}{n^2} e^{-(n\pi)^2 Fo'} \quad (13)$$

with  $Fo' = Fo \cdot \sqrt{t_{f,HE260B}/t_f}$  for R30, R60 and R90

$Fo' = Fo$  for R120

Eq. (13) was derived using the first four terms of the Fourier series. Hence the final value of the steel temperature is calculated with Eq. (14) for the three points given in Fig. 6. A fixed value for the thermal conductivity  $\lambda_a$  of 27.3 [W/mK] is used, Section 3.4.1.3 of [4].

$$T(X, Fo) = \theta'(X, Fo) \cdot q' \cdot H/\lambda_a + T_i \quad (14)$$

### 3.4 Validation of the developed method – temperatures

Eq. (12) is now fully determined to compute the temperatures on the three selected points. In the following graphs, the correlation between the analytical results and the values obtained by numerical simulation with SAFIR [9] for the sections given in Table 1 is presented, Fig. 8.

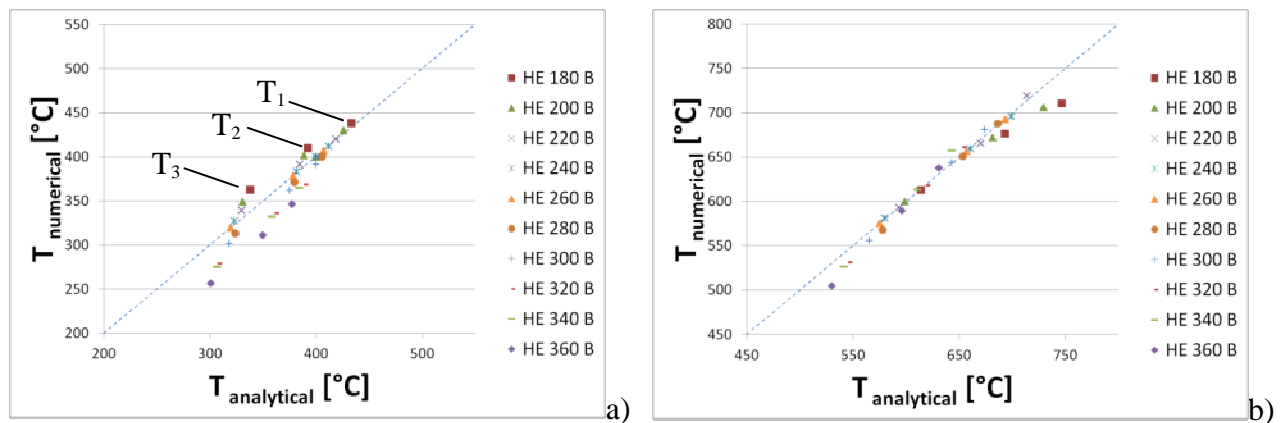


Fig. 8. Comparison of steel temperatures calculated with Eq. (12) and numerically a) R30; b) R60

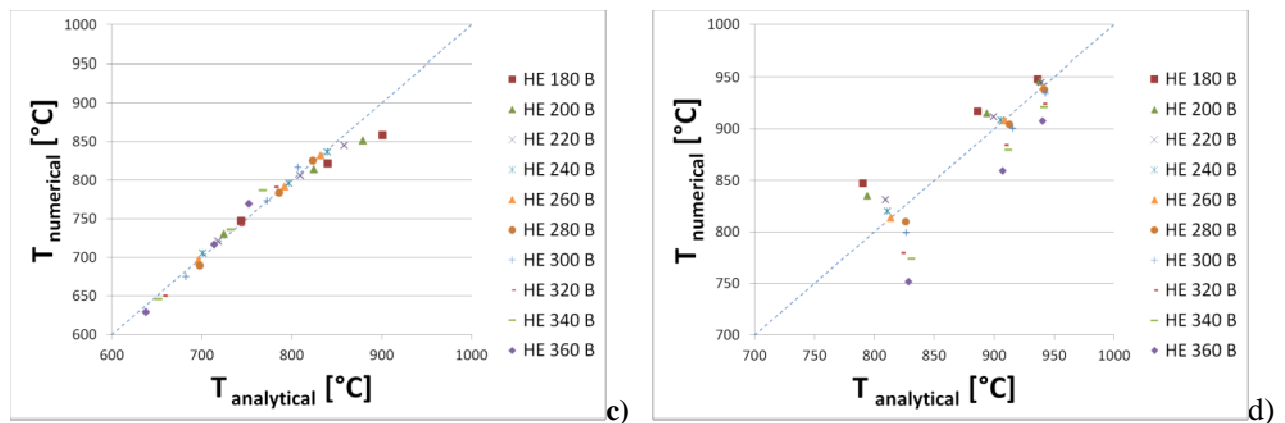


Fig. 8. Comparison of steel temperatures calculated with Eq. (12) and numerically c) R90; d) R120

Fig. 8 b) and c) show a very good correlation of the analytically and numerically calculated temperatures at R60 and R90. Also for R30 and R120 the average temperature of the plate (Point 1,  $T_1$ ) and the average temperature of the lower flange (Point 2,  $T_2$ ) are adequate. A bigger difference between the results is found for the average temperature in the root fillet (Point 3,  $T_3$ ). However, as the influence of the root fillet on the bending resistance is rather small, the difference of temperature in this point is considered acceptable, see Fig. 9.



The position of the 400°C limit is of significant interest for the calculation of the bending resistance, because a reduction of the yield strength for structural steel has not to be considered until this temperature is reached [4]. The position of the 400°C point in the web of the hot rolled section can be calculated from the following expressions:

$$\text{R30: } h_{400,R30} = -1.21 \cdot H^2 + 0.39 \cdot H \quad (15)$$

$$\text{R60: } h_{400,R60} = -0.68 \cdot H^2 + 0.50 \cdot H \quad (16)$$

$$\text{R90: } h_{400,R90} = -0.89 \cdot H^2 + 0.63 \cdot H \quad (17)$$

$$\text{R120: } h_{400,R120} = -1.05 \cdot H^2 + 0.74 \cdot H \quad (18)$$

with H measured in meters [m] according to Fig. 6.

### 3.5 Validation of the developed method – plastic bending resistance

The bending resistance has been computed considering a full plastic moment when the section of the slim-floor beam is fully yielded, applying the equilibrium of forces with respect to the neutral axis on the depth of the cross-section. The whole steel section is considered as the yield strength of steel in tension is equal to the yield strength in compression. Regarding concrete, only the part in compression is considered. For the steel web, the dimensional coordinate of the 400°C point has to be used to define a linear interpolation in terms of temperature between this point and the level of the root fillet at the lower part of the web. As shown in Sections 2 and 3 only the temperature gradient within the height of the cross section is considered analytically. Extensive numerical studies have shown that the assumption of a uniform temperature distribution in the plate and the lower flange – as it is obtained by the developed simplified analytical method – would in certain cases lead to an overestimation of the bending resistance, see also Fig. 2. Therefore a reduction factor  $\beta$  is introduced to the bending resistance  $M_{pl,Rd,fi}$  obtained by Eq. (14):

$$M'_{pl,Rd,fi} = M_{pl,Rd,fi} / \beta \quad (16)$$

where R30, R120:  $\beta = 1.25$

R60, R90:  $\beta = \sqrt{h/0.15}$  with h [m], Fig. 6.

In some cases the chosen formulation of the  $\beta$ -factor leads to very safe results (see Fig. 9a, e.g. HE360B for R30 and R60). But a simple formulation of the reduction allowing for an easy application of the derived method was preferred. For R60 and R90 a strong correlation to the height of the hot rolled section was found, which might be a subject for further investigations.

A comparison of the bending resistance of composite and non-composite SFB sections in fire  $M'_{pl,Rd,fi}$  with bending resistances derived by numerical simulation [9] is shown in Fig. 9.

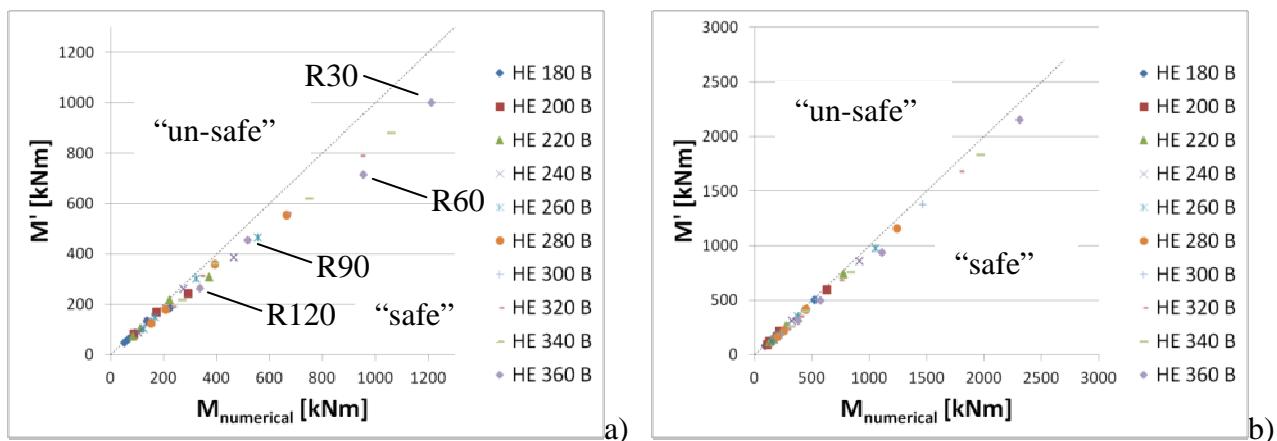


Fig. 9. Comparison of bending resistance a) non-composite cross section; b) composite cross section with  $b_{eff} = 1m$

The above presented comparison of  $M'$  with the numerically derived bending resistance in fire shows, that all values calculated with the developed simplified analytical method are conservative (“safe sided”) and further, that the developed method leads to very precise results for non-composite and composite cross sections. Additional parametric studies were performed with composite sections with participating widths up to  $b_{eff} = 3.0m$ .



#### 4 APPLICATION EXAMPLE

The application of the developed method is demonstrated in an example. For a hot rolled section HE200B + Plate 350x20mm in steel grade S355, the temperatures and the bending resistance in fire is calculated for 90min ISO-Fire (R90). The lower edge of the steel plate and the slab are exposed to the fire. The steel section is placed in a solid concrete slab in C30/37, a concrete cover above the upper flange of the hot rolled section of 50mm is used. A composite action between the steel section and the concrete is assured by means of “CoSFB-Betondübel” [6]. An effective width  $b_{\text{eff}} = 1.75\text{m}$  of the concrete slab is activated. Table 2 presents the calculated steel temperatures  $T$  for the three reference points in comparison to the temperatures obtained by numerical simulation  $T_{\text{num}}$  [9].

Table 2. Application Example – Temperature calculation for fire resistance class R90

Point	H [m]	z [mm]	X = x/H	q' [W/m <sup>2</sup> ]	$\lambda_a$ [W/mK]	Fo	$\Theta'(X,t)$	T [°C]	T <sub>num</sub> [°C]	$\Delta T$ [%]
1	0.22	10.00	0.05	67455	27.3	1.30	1.58	879	844	4.0
2	0.22	27.50	0.13	67455	27.3	1.25	1.48	825	806	2.3
3	0.22	53.00	0.24	67455	27.3	1.17	1.30	725	721	0.6

The position of 400°C in the web of the steel section is calculated using Eq. (17):

$$h_{400} = -0.89 \cdot H^2 + 0.63 \cdot H = -0.89 \cdot 0.22^2 + 0.63 \cdot 0.22 = 0.0955\text{m} = \mathbf{95.5\text{mm}}$$

(This value can be compared with the value obtained by numerical simulation  $h_{400,\text{num}} = 98.4\text{mm}$ ).

Based on the above calculated temperatures, the bending resistance of the SFB section for R90 can be derived. The yield strength of steel at elevated temperatures is calculated by multiplying the yield strength of structural steel  $f_y$  at room temperature by a reduction factor  $k_{y,\Theta}$ , Section 3.2 [4]. Annex F of [5] was applied for the calculation of the concrete compression force  $F_c$ . Subsequently the inner forces  $F_{\Theta,i}$  can be calculated. No external normal force is acting, so the position of the plastic neutral axis  $z_{\text{pl,fi}}$  can be found by the condition  $\Sigma F_{\Theta,i} = 0$ . Finally, the bending resistance is calculated by equilibrium with  $M'_{\text{pl,Rd,fi}} = \Sigma(F_{\Theta,i} \cdot z_{\text{pl,fi}}) / \beta$ , Fig. 10.

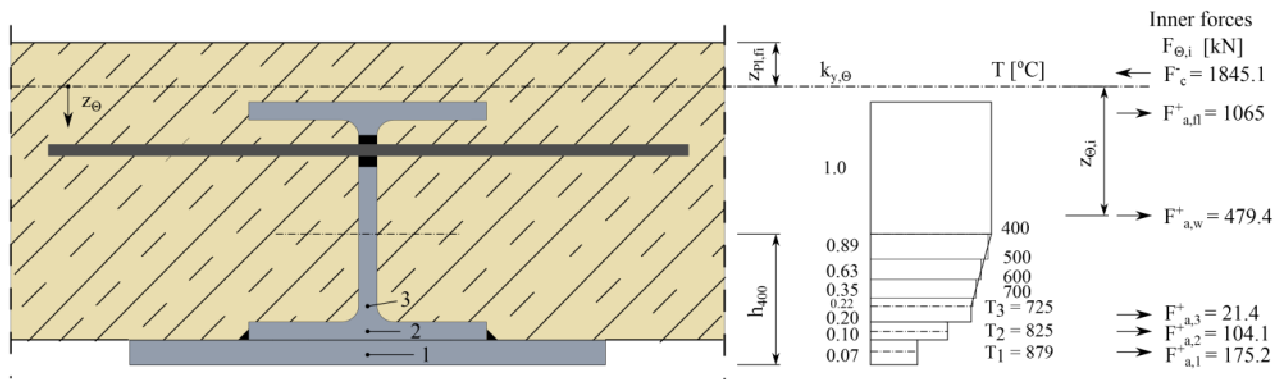


Fig. 10. Application example - Calculation of the bending resistance of a composite SFB cross section for R90

The position of the plastic neutral axis is calculated to  $z_{\text{pl,fi}} = \mathbf{41.35\text{mm}}$  (from the upper edge of the concrete slab downwards). Applying Eq. (16) the bending resistance at R90 is obtained:

$$M'_{\text{pl,Rd,fi}} = M_{\text{pl,Rd,fi}} / \beta = 159.3\text{kNm} / \sqrt{0.20/0.15} = \mathbf{138.0\text{kNm}} < 157.9\text{kNm} \text{ (Safir)}$$

A significant increase of the bending resistance  $M'_{\text{pl,Rd,fi}}$  can be achieved by adding reinforcement bars in the chamber of the hot rolled section in longitudinal direction of the beam span [10].

For the predesign of a CoSFB at room temperature for serviceability limit state (SLS) and for ultimate limit state (ULS) software is available [11].

## 5 CONCLUSION AND OUTLOOK

A simplified method to calculate the steel temperatures and bending resistances for SFB sections is presented. The developed method is based on the solution of the transient heat conduction equation for a section exposed to the standard temperature-time curve at one side and a constant gas temperature at the other side. It was shown that the developed method allows for a precise prediction of the average temperatures of the steel plate and the lower flange of the hot rolled section. Based on the derived temperature distribution the bending resistance for steel and steel-concrete composite cross sections can be calculated for R30, R60, R90 and R120 fire resistance classes. Finally the application of the method was demonstrated in an example.

To allow for a more general use of the developed method, additional parametric studies with variation of the steel grade, the concrete compression class and the height of the concrete cover above the upper flange have to be performed. Also the derived  $\beta$ -factor might be subject for further investigations. In addition the possible use of other slab types than a solid slab and more section types is still to be verified. The application of the developed approach for fire protected SFB sections will be given in another publication.

## REFERENCES

- [1] M. Braun, O. Hechler, V. Birarda: 140m<sup>2</sup> Column Free Space due to Innovative Composite Slim Floor Design. 9th International Conference on Steel Concrete Composite & Hybrid Structures. Leeds, UK, 2009.
- [2] M. Braun, R. Obiala, Chr. Odenbreit, O. Hechler: CoSFB – Design and Application of a new Generation of Slim-Floor Construction. 7th European Conference on Steel and Composite Structures. Naples, Italy, Eurosteel 2014
- [3] Deutsches Institut für Bautechnik: Allgemeine bauaufsichtliche Zulassung – ArcelorMittal Systemdecke Cofraplus 220. Zulassungsnummer Nr. Z-26.1-55, Berlin 2013
- [4] CEN European Committee for Standardization: EN 1993-1-2, Eurocode 3: Design of steel structures – Part 1-2: General rules – Structural fire Design. Brussels, 2005
- [5] CEN European Committee for Standardization: EN 1994-1-2, Eurocode 4: Design of composite steel and concrete structures – Part 1-2: General rules – Structural fire Design. Brussels, 2005
- [6] Deutsches Institut für Bautechnik: Allgemeine bauaufsichtliche Zulassung – ArcelorMittal Belval & Differdange S.A., CoSFB-Betondübel. Zulassungsnummer Nr. Z-26.4-59, Berlin 2014
- [7] Braun, M., Hechler, O., Hauf, G., Kuhlmann, U.: Embodied energy optimization by innovative structural systems. Final Conference of the COST Action C25: Sustainability of Constructions – Towards a better built environment. Innsbruck, Austria 2011.
- [8] CEN European Committee for Standardization: EN 1991-1-2, Eurocode 1: Actions on structures – Part 1-2: General actions – Actions on structures exposed to fire. Brussels, 2002
- [9] Franssen J.-M. SAFIR: A thermal/structural program for modeling structure under fire, A computer program for analysis of structures submitted to the fire. Engineering Journal, American Institute of Steel Construction Inc, Vol 42(3) (2005), pp143.
- [10] F. Hanus, D. Zaganelli, L.-G. Cajot, M. Braun: Analytical methods for the prediction of fire resistance of “reinforced” slim-floor beams. 8th European Conference on Steel and Composite Structures. Copenhagen, Denmark, Eurosteel 2017
- [11] ArcelorMittal R&D: ArcelorMittal Composite Slim-Floor Beams - CoSFB. ArcelorMittal Commercial Sections, Technical Advisory, 66 rue de Luxembourg, L-4009 Esch-sur-Alzette. [sections.arcelormittal.com](http://sections.arcelormittal.com)